Symposium on Predictive Capabilities in Environmentally Assisted Cracking
ASME Winter Annual Meeting
Miami, Florida
November 17-20, 1985

Influence of Small-Amplitude Cyclic Loading on Stress-Corrosion Cracking of High-Strength Steels in Salt Water

J. A. Hauser II and **T. W. Crooker**
Material Science and Technology Division
Naval Research Laboratory
Washington, DC 20375-5000

One of the primary characterization parameters for stress-corrosion cracking (SCC) of structural alloys is the threshold stress or stress-intensity below which SCC is not observed within a specified testing period. In fracture mechanics terminology, the SCC threshold parameter is termed K_{Iscc}. Threshold parameters are commonly measured under static loading conditions and are often regarded as a material/environment characteristic which can have general applicability for materials selection and structural design criteria. However, in recent years several investigators have shown that small-amplitude cyclic loading can significantly reduce the apparent SCC threshold in a variety of material/environment systems. The present investigation was undertaken to investigate this phenomenon using fracture mechanics test methods on two high-strength steels, 4340 and 5Ni-Cr-Mo-V, in 3.5 percent NaCl aqueous solution at ambient temperature and pressure.

K_{max} versus time-to-failure data were obtained using precracked cantilever-bend specimens under static loading and under small-amplitude cyclic loading with load ratios of R = 0.90 and 0.95 at a cyclic frequency of 0.1 Hz. In 4340 steel at the free corrosion potential and R = 0.90, preliminary tests showed no significant effect of cyclic loading on time-to-failure. In 5Ni-Cr-Mo-V steel, using zinc anodes to achieve an electrode potential of approximately -1.0 V (versus Ag/AgCl) to simulate cathodic protection, both time-to-failure and the apparent K_{Iscc} threshold were significantly reduced at R = 0.90 and reduced to lesser degree at R = 0.95. It is concluded that the statically-determined K_{Iscc} parameter can represent a nonconservative upper- bound measure of SCC sensitivity when applied to service conditions involving small-amplitude cyclic loading.

Introduction

Approximately 20 years ago, the application of fracture mechanics to stress-corrosion cracking (SCC) led to the development of the K_{Iscc} threshold parameter as a measure of SCC sensitivity in a particular material/environment system [1]. The use of fracture mechanics in SCC testing was regarded as being advantageous for several reasons: (i) the use of precracked specimens could eliminate the crack initiation period and thus reduce testing time; (ii) precracked specimens were found to be necessary to reveal SCC sensitivity in strongly passivating alloy/environment systems such as titanium in salt water; (iii) the use of fracture mechanics methods enabled results to be presented in terms of a geometry-independent threshold

parameter which could be directly translated from laboratory test specimen to structural configuration [2,3]. Thus, over the past two decades, the K_{Iscc} parameter has become accepted as a valid engineering measurement of SCC sensitivity and K_{Iscc} data appear in handbooks as a material property [4].

The K_{Iscc} parameter is normally measured in a quasi-static test. Although no formal test methods on K_{Iscc} testing have yet been published, generally accepted procedures involve either constant load or constant displacement tests. However in recent years, several investigators have reported that small-amplitude cyclic loading ("ripple-loading") can significantly reduce the apparent SCC threshold stress or stress-intensity in several alloy/environment systems [5-8]. These observations raise concern that, if the ripple-loading phenomenon is a general response of materials to SCC, then perhaps the quasi-static K_{Iscc} values which appear in handbooks may, in fact, be nonconservative upper-bound measures of SCC sensitivity.

This exploratory investigation was undertaken to examine the sensitivity of high-strength steels to SCC under ripple-loading conditions in salt water. The concern being addressed here is that high-strength steels are finding their way into critical applications on deep-water offshore structures where the principal loading involves sustained primary tensile forces with superimposed secondary small-amplitude cyclic loads caused by various effects resulting from ocean dynamics [9,10]. If ripple-loading effects are prevalent in the steel/salt water system, sensitivity to SCC in these structures could be seriously heightened in ways not measured by conventional K_{Iscc} testing.

Materials and Test Procedures

Two high-strength quenched-and-tempered structural steels were studied in this investigation, an AISI 4340 and a 5Ni-Cr-Mo-V. Chemical compositions and mechanical properties are given in Tables 1 and 2, respectively. Both materials were well characterized for static K_{Iscc} values in addition to undergoing ripple-loading studies.

All SCC tests were conducted using precracked cantilever-bend (CB) specimens, Figure 1. Precracking was conducted in general accordance with procedures recommended in ASTM E 399 [11], and the maximum stress-intensity (K_{max}) levels used in precracking were well below the K_{max} levels used in subsequent SCC tests. The stress-intensity expression used to calculate K_I values for the CB specimen is that given by Tada et al [12].

Static K_{Iscc} values were obtained under crack initiation conditions using deadweight loading. Specimens were loaded to discrete predetermined K_I values based on estimates of crack length obtained from loading compliance data. Ripple-loading time-to-failure data were obtained by using a simple system consisting of a motor-driven cam and springs to vary the deadweight loading in a controlled manner. The frequency of cyclic loading was 0.10 Hz, with a skewed triangular load-time waveform having a 9 second rise time and 1 second fall. This arrangement was chosen because cyclic loading in that range of frequencies can occur in large ocean structures and an abundance of evidence has been accumulated to show that many critical metal-environment

interactions tend to occur on the rise portion of the loading cycle when fresh metal surfaces are being produced. Ripple-loading data were obtained at two load ratio (minimum load/maximum load) values of R = 0.90 and 0.95, with one test on the 5Ni-Cr-Mo-V steel conducted at R = 0.925. Comparisons between static and ripple loading are made using common K_{max} values.

All SCC tests, with the exception of two tests on 4340 steel, were conducted in quiescent aqueous 3.5 percent NaCl solution at ambient temperature and pressure. Corrosion cells were placed so that the solution surrounded the notched-and-cracked center span of the CB specimen. The solution was replaced weekly and dissolved oxygen content was monitored daily. In two tests on 4340 steel, the solution was oxygenated to maintain a constantly saturated level of dissolved oxygen. Trends in dissolved oxygen content as a function of time are shown in Figure 2.

The 4340 steel specimens were tested at the free corrosion potential, and the 5Ni-Cr-Mo-V steel specimens were tested at a potential of approximately -1.0 V (versus Ag/AgCl) in order to simulate the effects of cathodic protection. In most tests involving cathodic polarization, a pair of zinc anodes were placed in the corrosion cell; however, a number of tests were conducted to compare results obtained using zinc anodes versus those obtained with an impressed current potentiostat device. Electrode potentials were monitored daily using a Ag/AgCl reference electrode.

Results

Initial K_I versus time-to-failure data for the 4340 steel are shown in Figure 3. Static SCC data are shown for both freely corroding and potentiostatically-controlled -1.0 V conditions. Also, the freely corroding data include two data points for statically-loaded specimens tested in oxygenated solution with dissolved oxygen levels maintained at 6 ppm, versus approximately 1 ppm for the quiescent solution. Two 4340 specimens were ripple-loaded at R = 0.90 under freely corroding conditions. Neither the oxygenation nor the ripple-loading appear to have had any significant effect on the time-to-failure data.

Initial K_I versus time-to-failure data for the 5Ni-Cr-Mo-V steel are shown in Figure 4. Here, most of the data were obtained from tests involving specimens coupled to zinc anodes. Under statically-loaded conditions, the apparent K_{Iscc} threshold using zinc anodes lies between 95 and 100 ksi$\sqrt{in}$. Under ripple-loading at R = 0.95, the time-to-failure data suggest an approximate order of magnitude reduction in time-to-failure. For R = 0.90, the time-to-failure data show a reduction of life of approximately two orders of magnitude less than that for static loading and a significant reduction in the apparent SCC threshold. Under R = 0.90 ripple-loading, specimens failed in less than 300 hours at a K_{max} levels as low as 75 ksi$\sqrt{in}$. An additional 5Ni-Cr-Mo-V specimen was tested at K_{max} = 100 ksi$\sqrt{in}$. and R = 0.925. Its time-to-failure failure fell midway between data points for R = 0.90 and 0.95 at the same K level, showing a distinct ordering on the basis of R ratio.

It is interesting to note that two specimens of the 5Ni-Cr-Mo-V steel were tested under ripple-loading using a potentiostat instead of zinc anodes. In both instances, these specimens failed after longer times than similarly-loaded specimens coupled to zinc anodes. This is counter to the comparison between zinc-coupled and potentiostatically-controlled specimens observed in 5Ni-Cr-Mo-V specimens under statically-loaded conditions, Figure 5.

Discussion

For many years, SCC was widely regarded as an essentially static failure process resulting from the combined action of sustained tensile stress and a corrosive environment. However, more recently, SCC and related corrosion fatigue mechanisms have come to be recognized as resulting from the combined action of localized plastic strain and strain rate [13]. The role of localized plastic strain is to provide preferential sites for cracking mechanisms such as hydrogen embrittlement or anodic dissolution to operate, and the role of strain rate is to disrupt the formation of oxide films on fresh metal surfaces which impede access of the corrosive environment to the crack tip. Thus, in these terms, SCC and corrosion fatigue can be seen as highly localized preferential corrosion processes which are promoted by small perturbations in strain equilibrium that are just sufficient to offset the chemical process of protective film formation.

Based upon recent experimental studies previously cited [5-8], small-amplitude cyclic loading can provide the type of strain perturbations

which are effective in promoting SCC. This finding is of considerable practical importance because, although most laboratory testing for SCC is conducted under quasi-static loading conditions, most loading in actual service conditions involves some degree of load perturbation from vibrational or other environmental forces. Thus, much laboratory SCC testing may, in fact, be producing materials characterization data which are fundamentally nonconservative.

The exploratory results presented in this paper would seem be bear out that concern for the steel/salt water system. However, the data presented here raise two questions which lie beyond the scope of the present study. First, are the results for the 5Ni-Cr-Mo-V steel simply a manifestation of corrosion-fatigue crack growth under high R-value loading, rather than some previously unrecognized SCC phenomenon? To address this concern, comparative near-threshold fatigue crack growth rate (da/dN versus ΔK) data would have to be generated in a salt water environment at high R values and at a low cyclic frequency. Such data are difficult and expensive to generate. Also, this type of crack growth data are often obfuscated by corrosion product formation within the crack. However, the K_{max} and R values involved in the 5Ni-Cr-Mo-V data definitely result in ΔK values which lie within the near-threshold crack growth rate regime.

Second, why did the two exploratory tests on 4340 steel fail to show any effects of ripple-loading? Here, it can only be pointed out that mechanistic

studies of mechanical/environmental interactions in SCC have shown numerous complexities involving the relative rates of film formation, loading and environmental attack. Thus, it is not surprising that possible ripple-loading effects are not necessarily recognized on the basis of a small sample of exploratory test data.

Conclusions

This exploratory study has demonstrated that small-amplitude cyclic loading can strongly affect the time-to-failure and K_{ISCC} threshold results obtained from stress-corrosion cracking tests on the steel/salt water system. Further study will be required to fully understand the significance of these findings. However, these results suggest that the traditional method of characterizing stress-corrosion cracking sensitivity in quasi-static laboratory tests may produce nonconservative results.

Acknowledgements

The authors wish to acknowledge the combined support of the Minerals Management Service and the David W. Taylor Naval Ship Research and Development Center in carrying out this research.

References

1 Brown, B. F., "A New Stress-Corrosion Cracking Test for High-Strength Alloys," *Materials Research & Standards*, Vol. 6, No. 3, March 1966, pp. 129-133.

2 Beachem, C. D. and Brown, B. F., "A Comparison of Three Precracked Specimens for Evaluating the Susceptibility of High-Strength Steel to Stress-Corrosion Cracking," *Stress Corrosion Testing*, ASTM STP 425, American Society for Testing and Materials, Philadelphia, 1967, pp. 31-40.

3 Shahinian, P. and Judy, R. W., Jr., "Stress-Corrosion Crack Growth in Surface-Cracked Panels of High-Strength Steels," *Stress Corrosion--New Approaches*, ASTM STP 610, American Society for Testing and Materials, Philadelphia, 1976, pp. 128-142.

4 *Damage Tolerant Design Handbook*, MCIC-HB-01R, Metals and Ceramics Information Center, Battelle Columbus Laboratories, Columbus, Ohio, December 1983.

5 Parkins, R. N. and Greenwell, B. S., "The Interface Between Corrosion Fatigue and Stress-Corrosion Cracking," *Metal Science*, August/September 1977, pp. 405-413.

6 Ford, F. P., "Relationship Between Mechanisms of Environmental Cracking and Design Criteria," Report No. 79CRD119, General Electric Company, Corporate Research and Development, Schenectady, New York, May 1979.

7 Ford, F. P. and Silverman, M., "Effect of Loading Rate on Environmentally Controlled Cracking of Sensitized 304 Stainless Steel in High Purity Water," *Corrosion-NACE*, Vol. 36, No. 11, November 1980, pp. 597-603.

8 Fessler, R. R. and Barlo, T. J., "Threshold-Stress Determination Using Tapered Specimens and Cyclic Stresses," *Environment-Sensitive Fracture: Evaluation and Comparison of Test Methods*, ASTM STP 821, American Society for Testing and Materials, Philadelphia, 1984, pp. 368-382.

9 Ellers, F. S., "Advanced Offshore Oil Platforms," *Scientific American*, Vol. 246, No. 4, April 1982, pp. 38-49.

10 Bortelho, D. L. R., Finnigan, T. D., Petrauskas, C., and Liu, S. V., "Model Test Evalution of a Frequency-Domain Procedure for Extreme Surge Response Prediction of Tension Leg Platforms," Paper No. OTC 4658, 16th Annual Offshore Technology Conference, Houston, Texas, May 7-9, 1984.

11 ASTM E 399 - 83, "Standard Test Method for Plane-Strain Fracture Toughness of Metallic Materials," *1984 Annual Book of ASTM Standards*, Section 3, Vol. 03.01, American Society for Testing and Materials, Philadelphia, 1984, pp. 519-554.

12 Tada, H., Paris, P. C., and Irwin G. R., *The Stress Analysis of Cracks Handbook*, Del Research Corporation, Hellertown, Pa., 1973.

13 Ford, F. P., "Current Understanding of the Mechanisms of Stress Corrosion and Corrosion Fatigue," *Environment-Sensitive Fracture: Evaluation and Comparison of Test Methods*, ASTM STP 821, American Society for Testing and Materials, Philadelphia, 1984, pp. 32-51

Table 1 - Chemical Composition (weight percent)

Material	C	Mn	P	S	Si	Cu	Ni	Cr	Mo	V
4340	0.41	0.74	0.01	0.016	0.21	--	2.00	0.74	0.26	0.05
5Ni-Cr-Mo-V	0.13	0.82	--	0.002	0.24	0.05	5.20	0.44	0.52	0.05

Table 2 - Tensile Properties

Material	0.2% Yield Strength (ksi)	Ultimate Tensile Strength (ksi)	Elongation in 2 in. (%)	Reduction in Area (%)
4340	180	190	12	40
5Ni-Cr-Mo-V	135	142	20	65

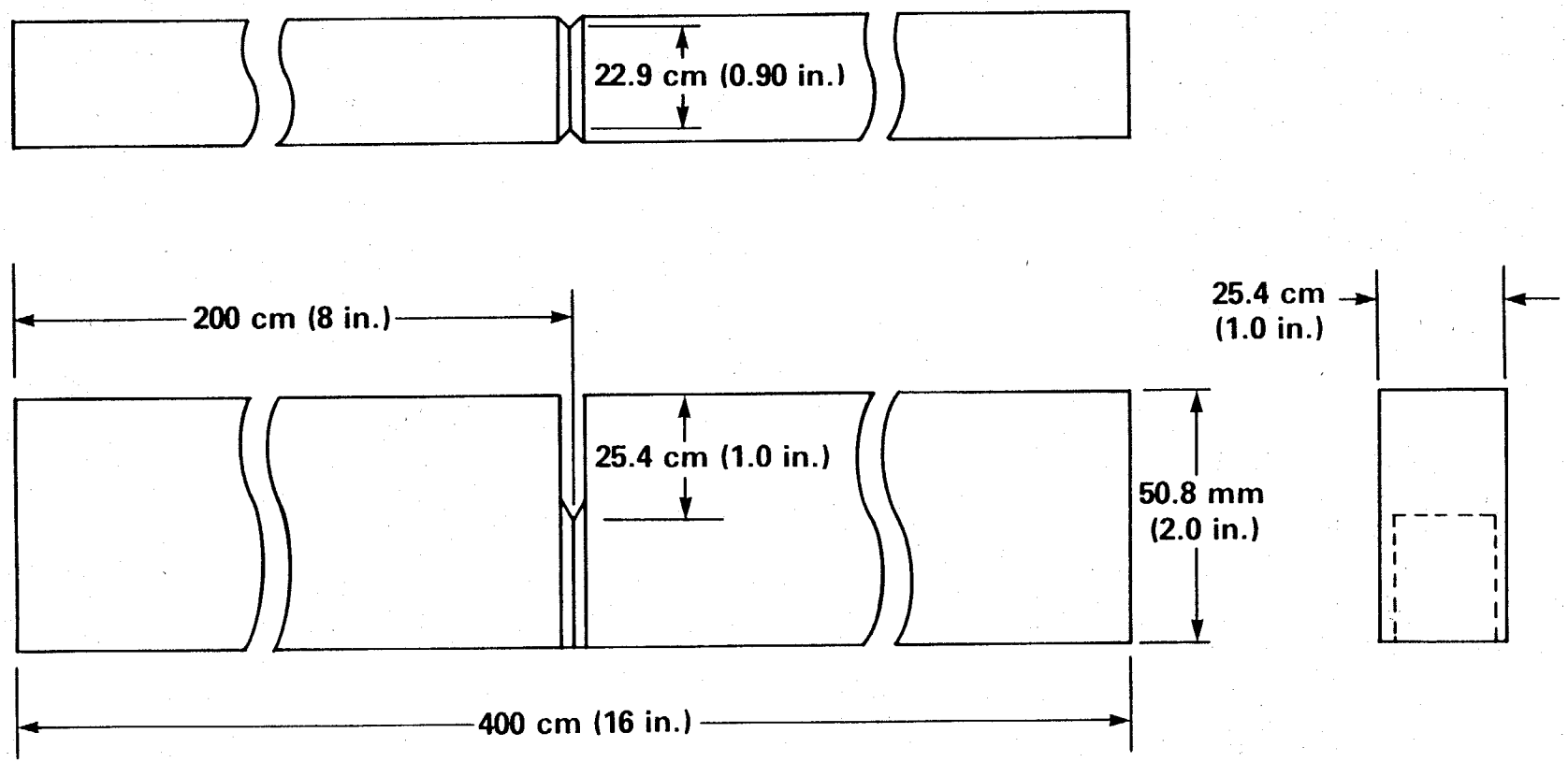

Figure 1 - Details of the precracked cantilever-bend (CB) stress-corrosion cracking test specimen.

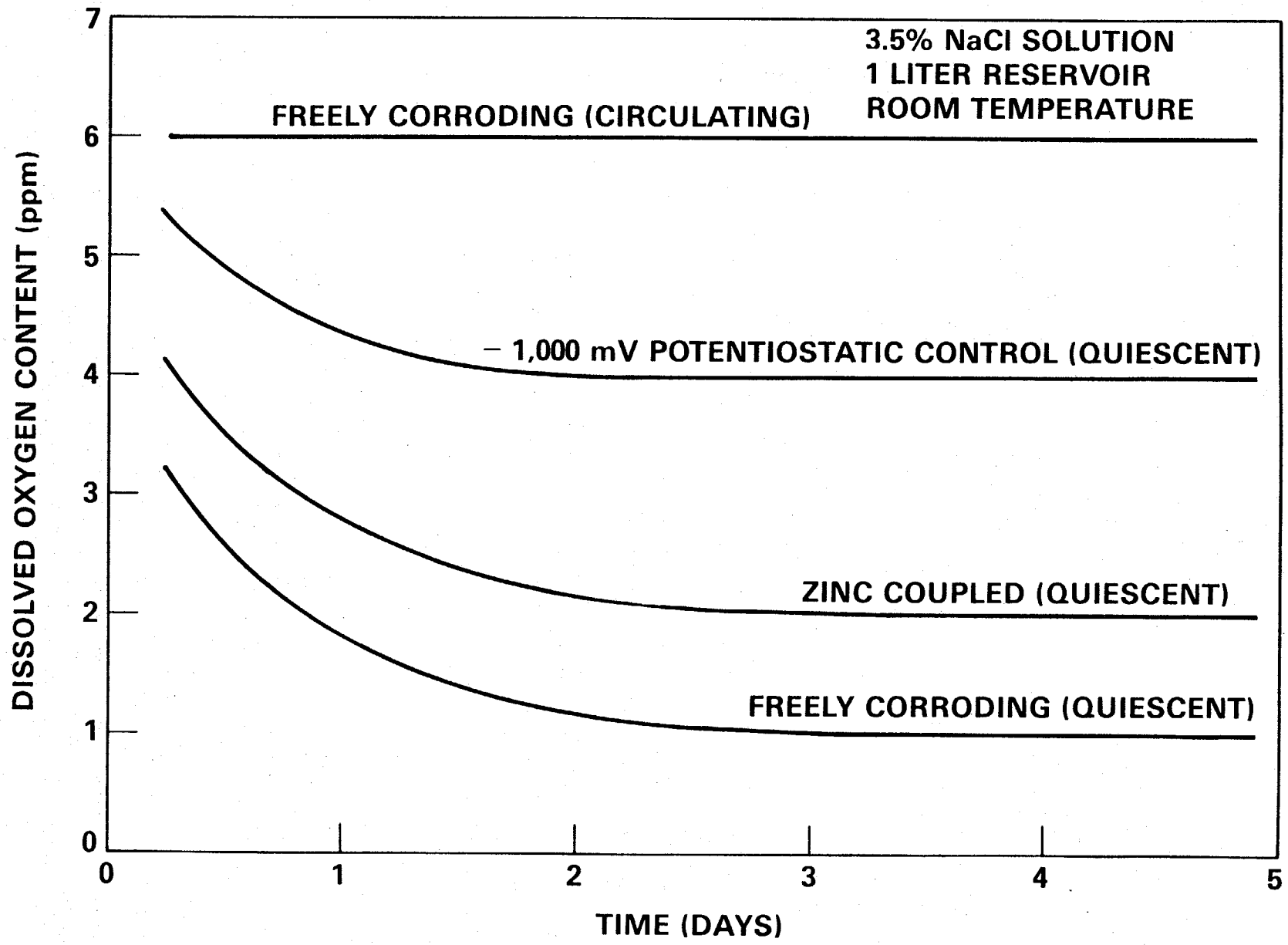

Figure 2 - . Trends in measured dissolved oxygen content as a function of time.

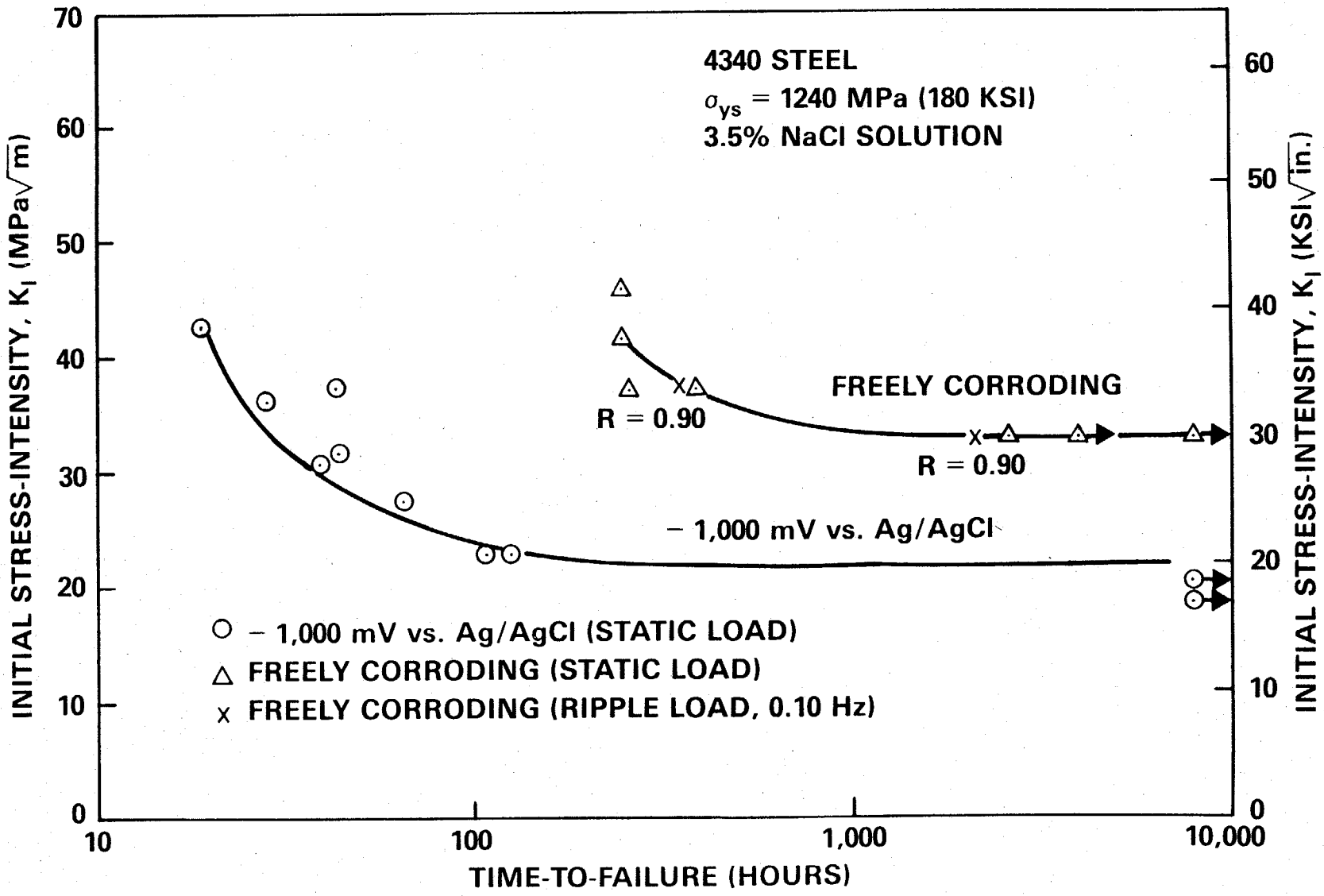

Figure 3 - Initial K_I versus time-to-failure data for the 4340 steel.

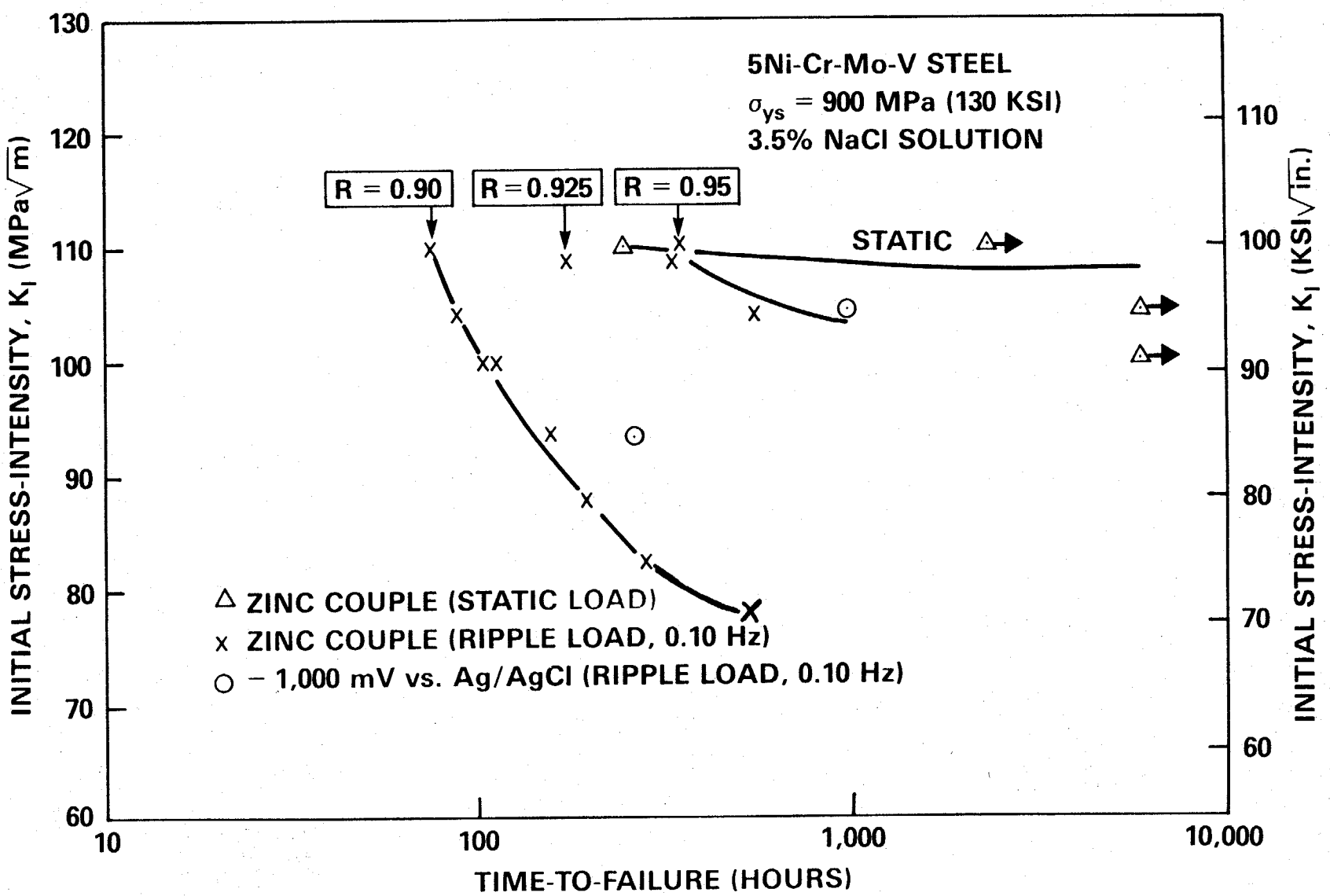

Figure 4 - Initial K_I versus time-to-failure data for the 5Ni-Cr-Mo-V steel.

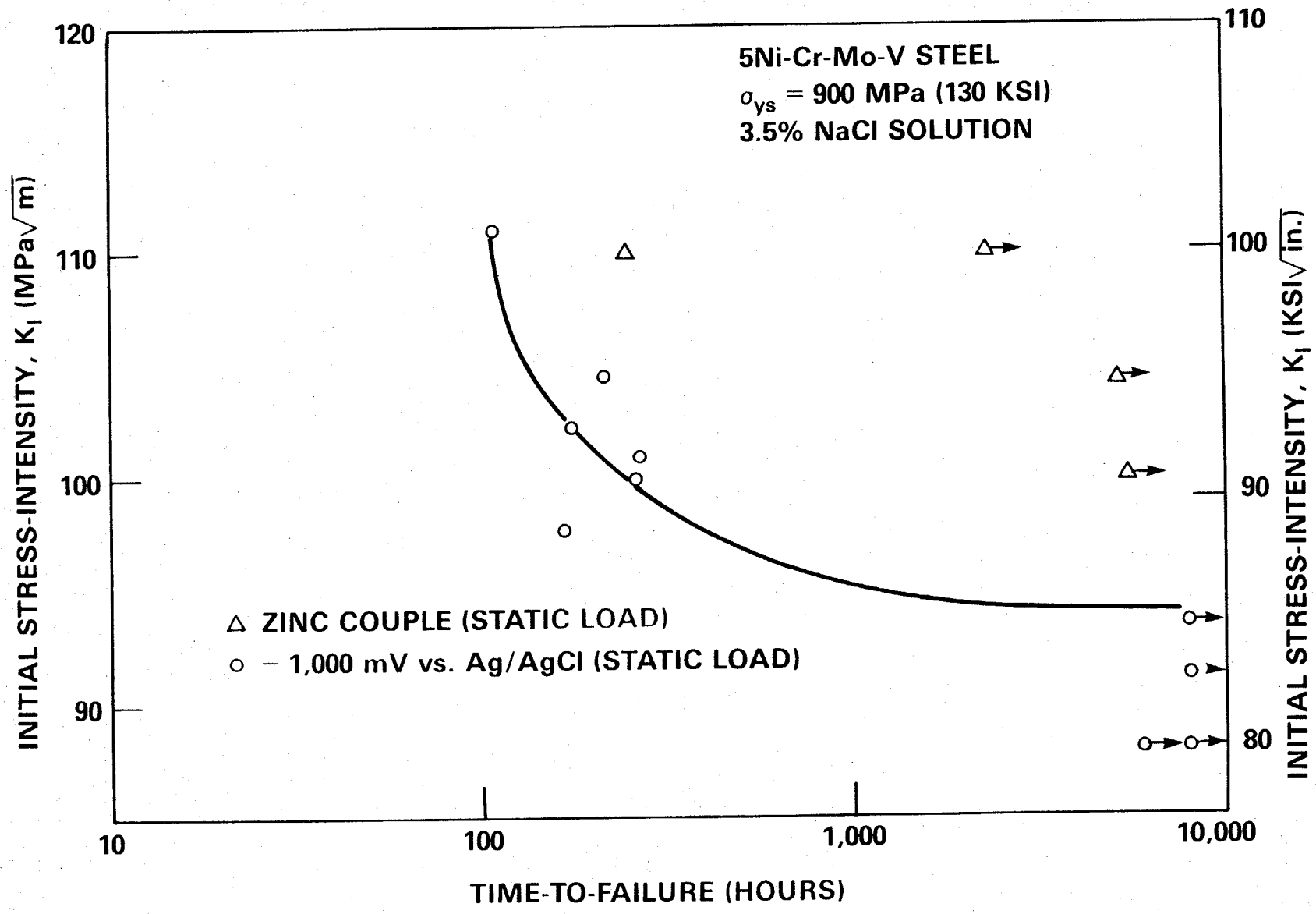

Figure 5 - Comparison of initial K_I versus time-to-failure for 5Ni-Cr-Mo-V steel comparing the effects of two methods of cathodic polarization.